Paula KURZAWSKA-PIETROWICZ (ID)

Combustion Engines
Polish Scientific Society of Combustion Engines

Comprehensive analysis of particle emissions from miniature turbojet engine

ARTICLE INFO

The emission of particulate matter from jet engines contributes to the deterioration of air quality in the vicinity of the airports and to the formation of contrails in higher layers of the atmosphere. This article presents the results of the measurements of particle emissions from a miniature jet engine GTM-120 fueled conventional aviation fuel Jet A-1. Analysis of particle size distribution, number, mass, and volume emission indexes has been made, as well as the analysis of the emission intensity and mass emission rate. The obtained results were related to LTO cycle phases. The results show that the particle number concentration was the lowest for low engine loads, with a characteristic diameter of 69.8 nm and a particle concentration of 7.7×10^6 particles/cm^3. For thrust increase, the characteristic diameter is smaller, and the particle distribution is no longer single-mode. The highest particle concentration for cm^3 is for 100% thrust and is equal to 1.55×10^7 particles, with a characteristic diameter of 34 nm.

1. Introduction

Nowadays, the emission of greenhouse gases from the aviation sector is one of the most important problem to be solved in the next years. In 2017, CO_2 emission from the aviation sector in the European Union was 3.8% of all emissions in the EU [6]. The adverse effects of air pollution on the health of the general public and the surrounding ecosystem have garnered significant attention at an international level [20]. As not only CO_2 emissions impact climate change, it is crucial to also reduce non-CO_2 emissions, such as nitrogen oxides, sulfur dioxide, and soot particles [14]. Soot particles emitted by aircraft engines have an impact on the formation of contrails under certain ambient temperatures and water vapor [5]. Pollution from aircraft affects both air quality and phenomena occurring in the upper layers of the troposphere during the cruise phase, but also contributes to significant environmental pollution during airport-related operations. Airport operation has a significant influence on air quality nearby. The main source of air pollution is aircraft operations, but there are much more polluters, such as ground support equipment, airport vehicles, fumes when refueling an aircraft, the use of de-icing substances, buses, and private cars traveling to the airport, and others [9]. Annex 16 to the Convention on International Civil Aviation describes the LTO cycle (Landing and take-off) used for the emission of carbon monoxide, nitrogen oxides, hydrocarbons, and non-volatile particles. The LTO cycle applies for engines with a maximum rated thrust greater than 26.7 kN and is calculated for operations made under 3000 ft [7]. The LTO cycle allows to calculate and assess the influence of aircraft activity on air pollution and air quality in the vicinity of the airport. Parameters of the LTO cycle are presented in Table 1. As particulate matter is one of the key pollutants causing smog in cities, it is important to understand its formation in engines better, especially jet engines.

According to actual studies, particles with aerodynamic diameters smaller than 0.1 μm are widely considered a health hazard [19]. Jet engines are dominated by particles with diameters smaller than 80 nm, which are produced by the nucleation mechanism. This mechanism involves the formation of particles during dilution and cooling of exhaust gases after entering the external surroundings. The particles produced in the nucleation process have a very low mass. Particles resulting from the accumulation phase have the largest mass share and have diameters ranging from 80 to 1000 nm. The agglomeration mechanism involves the absorption of the substances of the soluble fraction by soot agglomerates. Another mechanism of particle formation is the coarsening mechanism, which produces particles with diameters ranging from 2.5 to 40 μm. This mechanism involves the deposition of particles on the walls of the engine exhaust system, which are then torn off by the flowing exhaust gases [5, 18].

Table 1. Parameters of LTO cycle [7]

LTO phase	F_{max} [%]	Time [min]
Taxi	7	26
Landing	30	4
Climbout	85	2.2
Take-off	100	0.7

The particle emission from the jet engine covers non-volatile particles (nvPM) and volatile particles (vPM). Primary (non-volatile) particles are formed in the combustor of the jet engine and consist mainly of soot and other exhaust gas components that accumulate on the carbon core. Volatile particles condense and agglomerate in the exhaust plume or later disperse into the surrounding air. Volatile particles are formed as a result of the reaction of primary particulate matter and other toxic exhaust gas components, such as nitrogen oxides, sulfur oxides, and light hydrocarbons. Volatile particles are more difficult to measure and calculate, but more and more research is being done in this area to better understand how they arise and how to model them [18].

The certification standards for nvPM were set up in 2016 by the ICAO Committee on Aviation Environmental Protec-

tion (CAEP). The new standards require reporting of emission indexes of particle number and mass. Before the CAEP standards were set up for nvPM, the sole emission standard for particulate matter was the smoke number [10, 18].

This article focuses on the analysis of non-volatile particle emissions from miniature jet engine GTM 120 throughout the entire operating range. The tests were made for conventional aviation fuel Jet A-1 from 10% to 100% of the maximum engine thrust in steps of 10. Measurements of particle number concentration allowed us to calculate particle mass concentration and also emission indexes. The analyzes performed make it possible to refer to the particle size distribution and emission indexes of full-scale jet engines. As showed in some of the previous studies, the correlation analysis for ecological tests (concentration of harmful exhaust compounds) based on Pearson's linear correlation coefficient between miniature jet engines and high-thrust engines was strong [16]. According to this research, it can be concluded that a similar nature of changes in concentration of harmful exhaust compounds in exhaust gases can be observed for miniature and high-thrust engines. More research focusing on the correlation between miniature engines and full-scale engines is needed to determine whether there is also a correlation between particulate matter concentrations. Due to the fact that emission tests on miniature engines are much more economical and easier to repeat, it is important that ecological analyzes using them can be applied to full-size engines.

2. Methods

The test was carried out on a miniature turbine engine, GTM-120, produced by JETPOL company. The engine has a single-stage radial compressor, diffuser, annular combustion chamber with a set of evaporators, turbine nozzle, turbine wheel, and nozzle cone. An illustrative diagram of GTM engines is shown in Fig. 1 [1]. The length of the engine is 340 mm, the width is 115 mm, and the weight is 1.5 kg. The parameters of the GTM-120 are shown in Table 2. The fixed research and measurement facility incorporates an extra pneumatic ignition system along with an electronic control and data logging system designed for the GTM-120 engine. This form of internal configuration of GTM-120 continues to be utilized in APUs or in simplified propulsion systems designed for unmanned aerial vehicles [2].
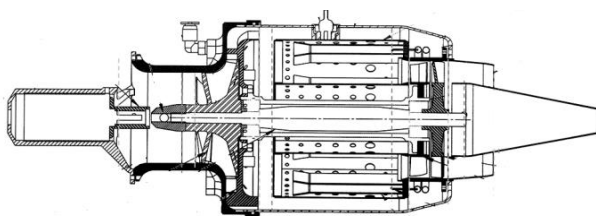
Fig. 1. Illustrative diagram of GTM-120 [1]

Table 2. Selected parameters of miniature turbine engine GTM-120

Parameter	Unit	Value
Maximum thrust	N	100
Fuel consumption for maximum thrust	g/min	520
Engine mass	kg	1.5
Engine length	mm	340
Engine width	mm	115

The EEPS 3090 (Engine Exhaust Particulate Sizer™ spectrometer) analyzer from TSI Incorporated was used to measure the particle number concentration in the exhaust. The measurement probe was placed at a distance of 30 cm from the engine outlet and the probe was made of stainless steel, which is non-reactive in high temperatures. Due to the use of an exhaust gas diluent, the exhaust gases in the tested sample constituted 3%. The total flow of the dilution system was 10 l/min. The EEPS 3090 analyzer measure the particles from 5.6 nm to 560 nm. Analyzer has 16 channels per decade, and the resolution is 10 Hz. The exhaust sample volume flow rate is equal to 0.6 m^3/h, and the compressed air volume flow rate is equal to 2.4 m^3/h. The temperature of the input sample is from 10 to 52^oC [17]. Also, the cyclone was used in the EEPS 3090, so the tested sample was cleaned of large particles and fibers, which could cause excessive noise on one or more channels [12].

The measuring range was from 10 to 100% of the maximum thrust, every 10. The diagram of the measurement station is shown in Fig. 2.
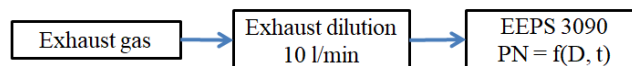
Fig. 2. Diagram of the measurement station

The results were analyzed using particle number concentration and particle size distribution (PSD), which allowed the calculation of the particle mass concentration using the unit density of the particles according to a specific model [3]. Also, the emission indexes for the number, mass, and volume of particles have been calculated.

The data collected by the EEPS was averaged based on identical fuel flow rate conditions and subsequently transformed into a differential number-based (dEI_N/dlogD), mass-based (dEI_M/dlogD) and volume-based (dEI_V/dlogD) distribution of particle sizes. Number-based particle size distribution was calculated based on the particle number concentration multiplied by fuel flow and divided by fuel consumption. The mass-based and volume-based particle size distributions were calculated in the same way, using particle mass concentration and particle volume concentration instead of particle number concentration.

3. Results and discussion

The concentration of particles measured by EEPS 3090 was analyzed and calculated on emission indexes to compare it with other studies. The number concentration of particles is shown in Fig. 3. Dominate the particles with diameters from about 20 nm to 125 nm, which is characteristic of jet engines. The particle distribution changes with thrust increase. For 10 N, the distribution is single-mode and has the lowest particle concentration from tested points with a characteristic diameter of 69.8 nm, and the particle concentration for 69.8 nm diameter is 7.7×10^6 particles/cm^3. For thrust increase, the characteristic diameter is smaller, and the particle distribution is no longer single-mode. For high engine loads, from 60% to 100%, the distribution is slightly different for every measurement point but the shape of the distribution is very similar. From 60% of thrust, there are also more particles with diameters from about 7 nm to

12 nm, with a peak diameter of 9.31 nm. The highest particle concentration for cm^3 is for 100% thrust and is equal to 1.55×10^7 particles, with a characteristic diameter of 34 nm.

The mass concentration of particulate matter is shown in Fig. 4. The distribution is log-normal single mode. The center of the nucleation mode peaks for every measurement point is 80–100 nm depending on the thrust. The dominant particulate matter is for 10 N and 40 N, where the peak value exceeds 1200 mg/m^3. For other measurement points, the value of the peak is about 900–1000 mg/m^3 and decreases with the increase of thrust. There is also a slight increase in the mass concentration of particles with a diameter larger than 100 nm at every point of thrust.
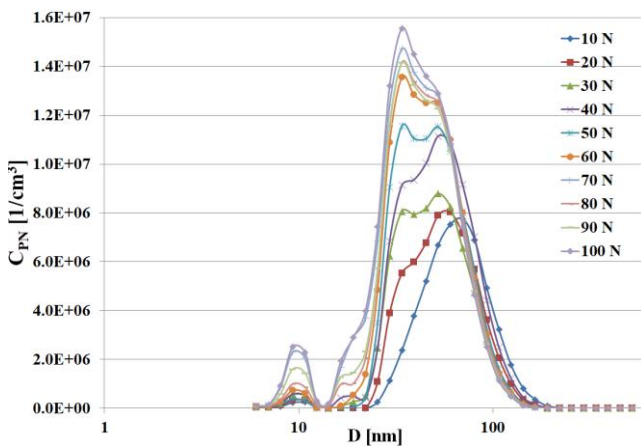
Fig. 3. Particles number concentration for measurement points
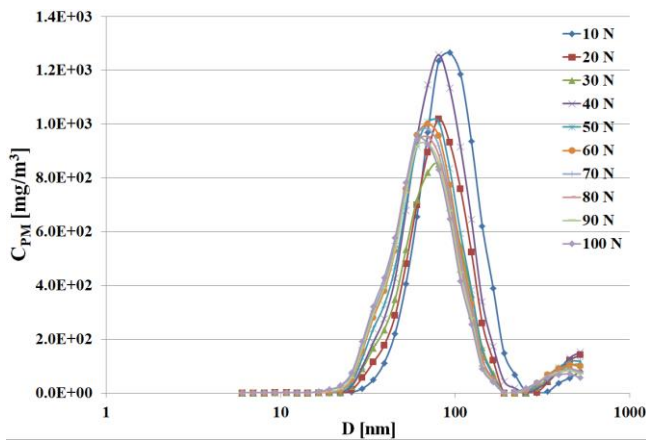
Fig. 4. Particles mass concentration for measurement points

Based on the data obtained, the intensity of the number of particles was determined for each measurement point. The intensity of the number of particles is an index calculated based on the particle number concentration and volume flow rate of exhaust gases. The intensity of the number of particles is shown in Fig. 5. It can be seen that the PM number emission intensity mostly increases with an increase of thrust and has the highest value for 100 N, which is equal to 4.1×10^{13} particles/s. The mass emission rate in grams per hour is shown in Fig. 6. The general trend is also

increasing with increasing thrust and has the maximum value of 8.5 g/h for maximum tested thrust.
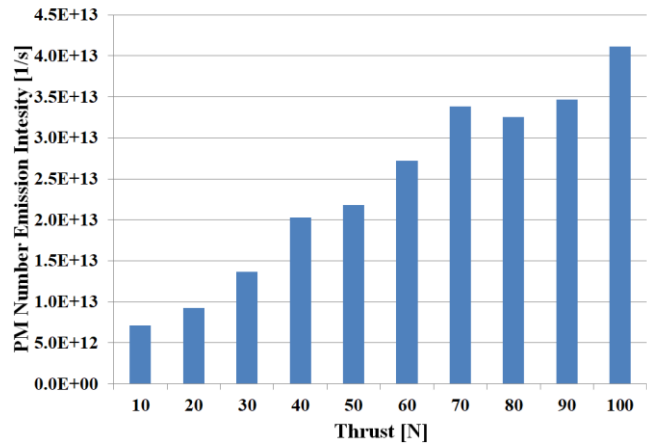
Fig. 5. Intensity of particles number emission
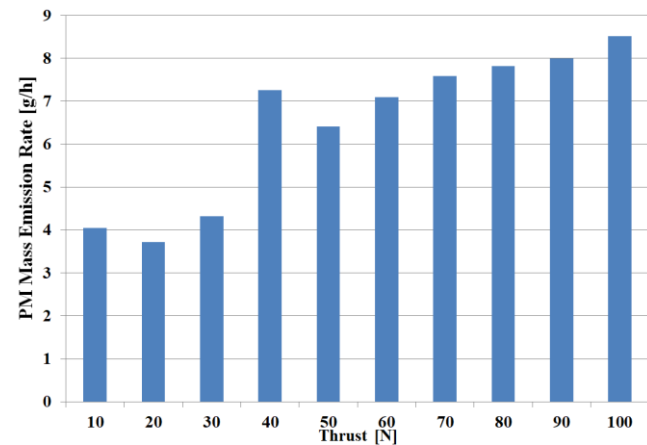
Fig. 6. PM mass emission rate

Figure 7 presents the particle number emission index for each measurement point. The emission is the highest for 70 and 100% of engine thrust and is about 9.5×10^{15} particles per kg of fuel, and the lowest for 10% of engine thrust, which is equal to 5.1×10^{15} particles per kg of fuel. Figure 8 presents the PM mass emission index.
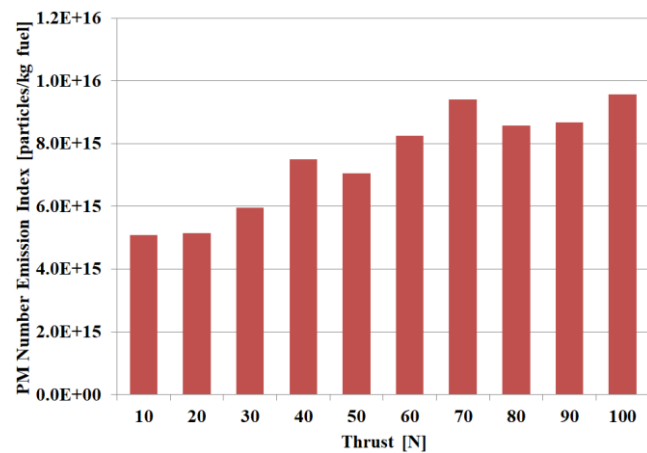
Fig. 7. PM number emission index

Fig. 8. PM mass emission index
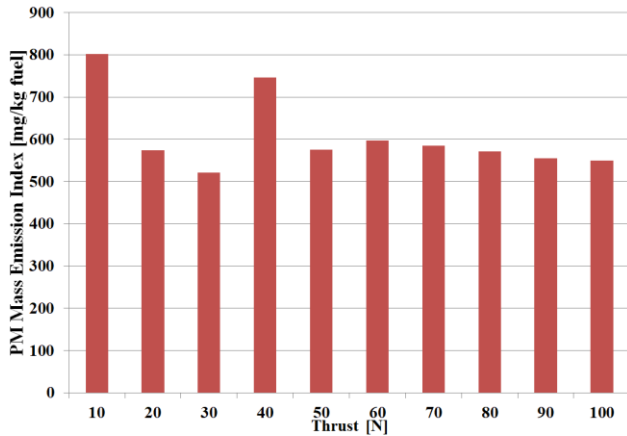
Fig. 10. Mass-based particle size distribution

The number-based particle size distribution ($dEI_N/dlogD$) is shown in Fig. 9. EI_N is the number of particles calculated on the unit mass of the fuel. Geometric mean diameter (GMD) decreases with the increase in thrust. GMD starts from 69.8 nm for 10 N, and from 50 N to 100 N is constant and equal to 34 nm. Comparing the GMD with other studies on full-scale engines, the results of GMD are different for miniature jet engines [4, 15]. For full-scale engines, the GMD increase with thrust increase, starting from about 15 nm for 10% of maximum thrust, and for high engine loads, from about 60% of thrust to the maximum thrust, the geometric mean diameter is about 35 nm [15].

The mass-based particle size distribution ($dEI_M/dlogD$) is shown in Fig. 10. EI_M is the mass of particles calculated on unit mass of the fuel in [µg/kg fuel]. The highest emission index is for 10% (93.1 nm) and 40% (80.6 nm), relatively 1.2×10^5 and 1.07×10^5 µg/kg fuel. The lowest characteristic diameter is for 30% of thrust (80.6 nm) and the EI_M is about 7.3×10^4 µg/kg fuel. Besides 30% of thrust, the lowest characteristic diameter is for thrust higher than 60% and is equal to 69.8 nm, for which the mass emission index is between 7.5–8.1 × 10^4 µg/kg fuel.

The volume-based particle size distribution ($dEI_V/dlogD$) is shown in Fig. 11. EI_V is the volume of particles calculated on a unit of the fuel in [mm³/kg fuel]. The magnitude of the EI_V in soot mode was the highest for 20 and 40% of thrust and the lowest for 100% of thrust. Particles in a soot mode arise due to coagulation and condensation of aromatic hydrocarbons and sulfur [11]
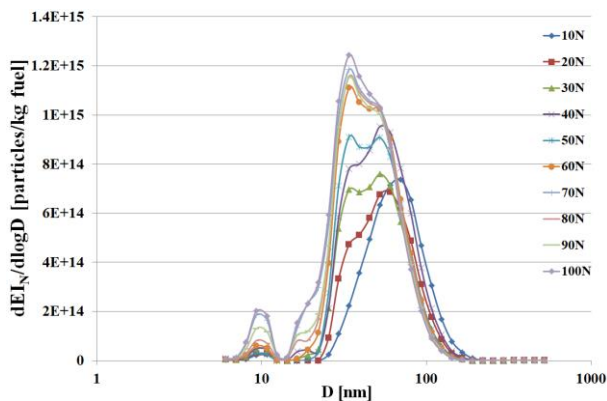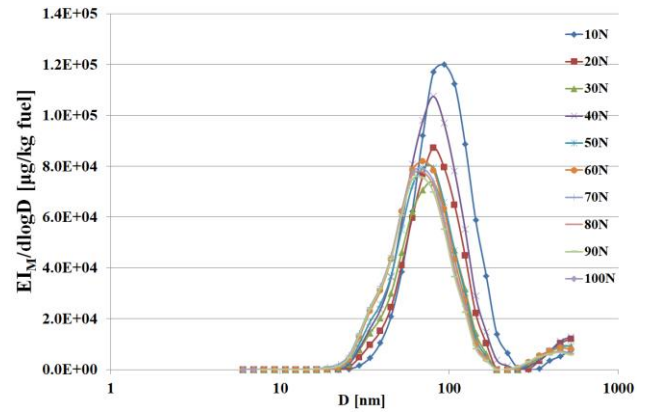
Fig. 11. Volume-based particle size distribution

Figures 12–16 show cumulative values of the relative number and relative mass of particles. The cumulative curves were established by normalizing the collected data for both the number and mass of particles to a value of 1. This was achieved by considering the ratio of the particle number to the maximum particle number, along with the ratio of particle mass to the maximum particle mass.

Figure 12 shows results for 10 and 20% of the thrust, where 90% of the relative number of all emitted particles is about 62% of their relative mass for 10 N, and 60% for 20 N.

The cumulative values for 30 and 40% of the thrust are shown in Fig. 13. The cumulative values of the relative number and relative mass shows that 90% of the relative number of all particles emitted is about 58% of their mass for 30 N and about 60% for 40 N.

The cumulative values for 50 and 60% of the maximum engine thrust is presented in Fig. 14. The cumulative values of the relative number and relative mass shows that for 50 N the 90% of the relative number of all particles emitted is about 60% of their mass and for 60 N the 90% of particles emitted is about 58% of their mass.

Figure 15 shows cumulative results for 70 and 80% of the maximum engine thrust. In both cases the 90% of the relative number of all particles emitted is about 57% of particles mass.

The cumulative values for 90 and 100% of the maximum engine thrust are shown in Fig. 16. In this case also,

Fig. 9. Number-based particle size distribution

the 90% of the relative number of all particles emitted is about 59% of their mass for 90 N and 58% for 100 N.

Relating the obtained results to other studies [13], the cumulative values of the relative number and relative mass of particles are 90% of the relative number of all emitted particles and 60% of their relative mass for every engine load, so obtained results are very close to other studies.
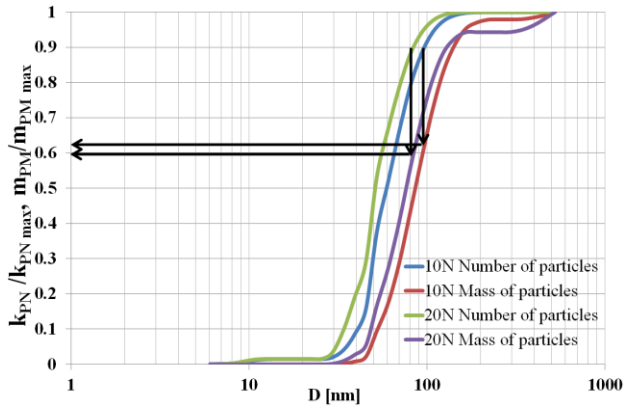
Fig. 12. Cumulative values of the relative particles number and relative mass of particulate matter for 10 N and 20 N
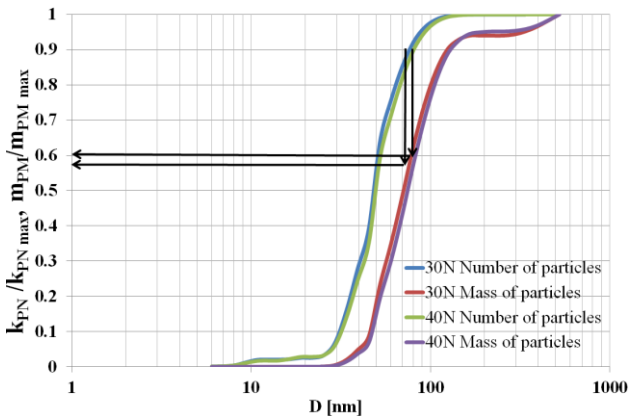
Fig. 13. Cumulative values of the relative particles number and relative mass of particulate matter for 30 N and 40 N
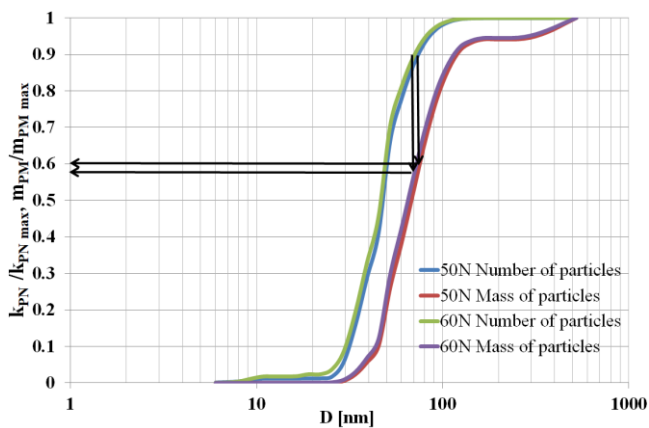
Fig. 14. Cumulative values of the relative particles number and relative mass of particulate matter for 50 N and 60 N
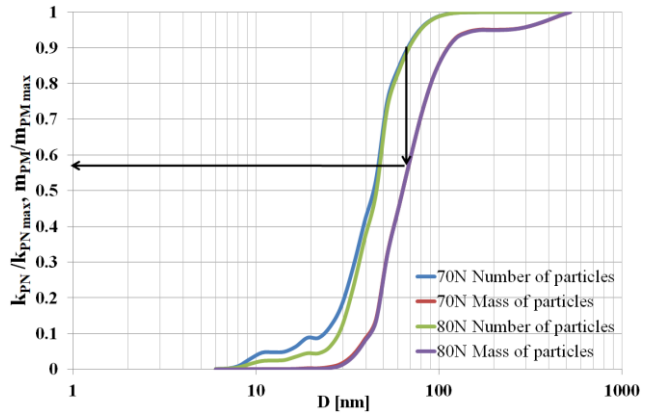
Fig. 15. Cumulative values of the relative particles number and relative mass of particulate matter for 70 N and 80 N
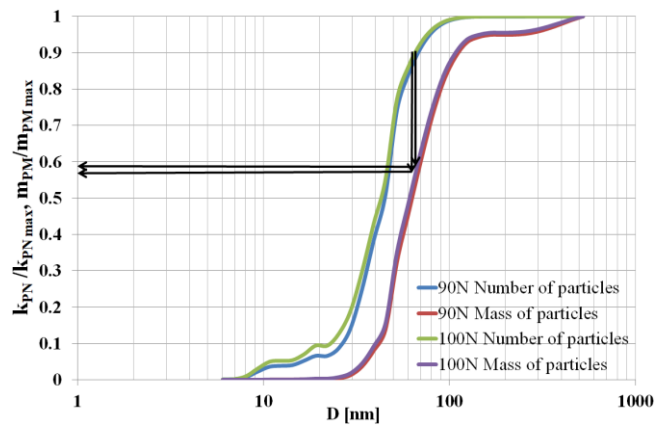
Fig. 16. Cumulative values of the relative particles number and relative mass of particulate matter for 90 N and 100 N

As the geometric mean diameter of particles from jet engines typically ranges from 15 nm to 60 nm [18], obtained results from miniature jet engine GTM 120 meet these ranges for almost every tested engine load. Only for 10 of the maximum thrust, the GMD is bigger than 60 nm and is equal to 69.8.

The LTO cycle describes the duration time of each operation phase and the percentage setting for maximum thrust for jet engines. The longest-lasting phase is taxiing, which, according to LTO, lasts 26 min, with a thrust force around 7% of the maximum. In the carried-out tests, only 10% of the maximum thrust was analyzed, but as it is a very low engine load, it can be referred to as the taxi phase. As showed the results, 10% of the maximum thrust has the highest value of the particle mass concentration, with a maximum value of 1266 mg/cm^3 for a diameter of 93.1 nm and a mass emission index of 800 mg for kg of fuel. For 10% of the maximum thrust, also the particle volume emission index is the highest, with a maximum value of 200 mm^3/kg fuel for the diameter of 107.5 nm. For particle number emission intensity, the 10% of maximum thrust has the lowest value, but taking into consideration the duration time of this phase, the number emission of particles during the taxi phase is the highest from other phases. The shortest phase in the LTO cycle is the take-off phase, which has the time of 0.7 min for 100% of thrust. The re-

sults for these phases show that the particle number intensity is the highest from all measurement points and is equal to 4.11×10^{13} particles per second, but as mentioned above, the duration time of this phase is very low, so the total number of particle emission will be significantly lower than for taxi phase.

4. Conclusions

As the airport activity is responsible for air pollution nearby and has a significant impact on air quality, the reduction of pollutions from airports is required. The main source of pollution from airport activity is aircraft operations, which emit greenhouse gases, toxic exhaust gas compounds such as CO, HC, NO_x, SO_x, and particulate matter, which contribute to the formation of smog in the cities. Also, the cruise phase of the aircraft contributes to air pollution and climate changes, as the nitrogen oxides affect radiative forcing [8]. Soot particles emitted by aircraft engines have an impact on the formation of contrails in higher layers of the atmosphere. As the airport-related operations affect ambient air quality, the calculation methods for main pollutants are described by the LTO cycle.

The particle size distribution changes with thrust increase. For particle number concentration, the values are the lowest for low engine loads and the highest for high engine loads. The longest-lasting phase of the LTO cycle is taxiing, which has the greatest impact on pollution near the airport, which was mentioned in the analysis. Even though

the number concentration of the particles was the lowest for low engine loads, considering the time of the taxi phase, the emission in this phase is much higher than for the take-off phase, which has the highest number concentration of particles. The highest mass emission index is for 10% of the maximum thrust for the diameter of 93.1 nm and 40% of the maximum thrust for the diameter of 80.6 nm, relatively 1.2×10^5 and 1.07×10^5 µg/kg fuel. The lowest characteristic diameter is 30% of the maximum thrust for the diameter of 80.6 nm, and the EI_M is about 7.3×10^4 µg/kg fuel. The magnitude of the EI_v in soot mode was the highest for 20 and 40% of thrust and the lowest for 100% of thrust. As shown in the graphs of cumulative values of the relative particle number and relative mass of particulate matter, 90% of the relative number of all particles emitted is from 57 to 62% of their mass, depending on the engine thrust.

It's important to highlight that the emission factor values provided for mass and number concentration haven't undergone adjustments for particle losses that vary with size in sampling systems and measurements. This presents another challenge in accurately estimating the quantity and mass of particulate matter emitted from jet engines. More research focusing on particle loss analysis should be performed and research on particles from miniature jet engines should be expanded to include the study of volatile particles generated at some distance from the engine.

Nomenclature

CO	carbon monoxide	HC	hydrocarbons
CO_2	carbon dioxide	LTO	landing and take-off
C_{PM}	particles mass concentration	nvPM	non-volatile particulate matter
C_{PN}	particles number concentration	NO_x	nitrogen oxides
EI_M	particle mass emission index	PM	particulate matter
EI_N	particle number emission index	PSD	particle size distribution
EI_V	particle volume emission indes	SO_x	sulfur oxides
F_{max}	maximum engine thrust	vPM	volatile particulate matter

Bibliography

[1] Chmielewski M, Gieras M. Small gas turbine GTM-120 bench testing with emission measurements. Journal of KONES Powertrain and Transport. 2015;22(1). https://doi.org/10.5604/12314005.1161610

[2] Czarnecki ML, Lech A. GTM-120 micro gas turbine engine noise identification. Combustion Engines. https://doi.org/10.19206/CE-189743

[3] Durdina L, Brem BT, Abegglen M, Lobo P, Rindlisbacher T, Thomson KA et al. Determination of PM mass emissions from an aircraft turbine engine using particle effective density. Atmos Environ. 2014;99:500-507. https://doi.org/10.1016/j.atmosenv.2014.10.018

[4] Durdina L, Brem TB, Schönenberger D, Siegerist F, Anet JG, Rindlisbacher T. Nonvolatile particulate matter emissions of a business jet measured at ground level and estimated for cruising altitudes. Environ Sci Technol. 2019;53(21): 12865-12872. https://doi.org/10.1021/acs.est.9b02513

[5] EASA. Updated analysis of the non-CO_2 climate impacts of aviation and potential policy measures pursuant to the EU Emissions Trading System Directive Article 30(4), 2020.

[6] European Commission. Reducing emissions from aviation. https://climate.ec.europa.eu/eu-action/transport/reducing-emissions-aviation_en

[7] Galant-Gołębiewska M, Jasiński R, Ginter M, Maciejewska M, Nowak M, Kurzawska P. Methodical aspects of the LTO cycle use for environmental impact assessment of air operations based on the Warsaw Chopin airport. Aviation. 2021; 25(2):86-91. https://doi.org/10.3846/aviation.2021.14972

[8] Grewe V, Dahlmann K, Matthes S, Steinbrecht W. Attributing ozone to NO_x emissions: implications for climate mitigation measures. Atmos Environ. 2012;59:102-107. https://doi.org/10.1016/j.atmosenv.2012.05.002

[9] ICAO Airport Air Quality Manual, Doc 9889, 2016.

[10] ICAO International Standards and Recommended Practices, Annex 16 to the Convention on International Civil Aviation, Environmental Protection: Volume II – Aircraft Engine Emissions, 4th ed.; ICAO: Montreal 2017.

[11] Jasiński R, Kurzawska P, Przysowa R. Characterization of particle emissions from a DGEN 380 small turbofan fueled with ATJ blends. Energies. 2021;14(12):3368. https://doi.org/10.3390/en14123368

[12] Jasiński R, Przysowa R. Evaluating the impact of using HEFA fuel on the particulate matter emissions from a turbine engine. Energies. 2024;17(5):1077. https://doi.org/10.3390/en17051077

[13] Kurzawska P, Jasiński R. Overview of sustainable aviation fuels with emission characteristic and particles emission of the turbine engine fueled ATJ blends with different percentages of ATJ fuel. Energies. 2021;14:1858. https://doi.org/10.3390/en14071858

[14] Kurzawska-Pietrowicz P, Maciejewska M, Jasiński R. Exhaust emissions from a jet engine powered by sustainable aviation fuel calculated at various cruising altitudes. Combustion Engines. 2024;198(3):62-67. https://doi.org/10.19206/CE-186211

[15] Lobo P, Durdina L, Brem BT, Crayford AP, Johnson MP, Smallwood GJ et al. Comparison of standardized sampling and measurement reference systems for aircraft engine non-volatile particulate matter emissions. J. Aerosol Sci. 2020; 145:105557. https://doi.org/10.1016/j.jaerosci.2020.105557

[16] Merkisz J, Jasiński R, Łęgowik A, Olejnik A. Exhaust emissions of jet engines powered by biofuel. Transport Problems. 2021;16(4):199-206. https://doi.org/10.21307/tp-2021-071

[17] Merkisz J, Pielecha J. The on-road exhaust emissions characteristics of SUV vehicles fitted with diesel engines. Combustion Engines. 2011;145(2):58-72. https://doi.org/10.19206/CE-117103.

[18] Owen B, Anet JG, Bertier N, Christie S, Cremaschi M, Dellaert S et al. Review: particulate matter emissions from aircraft. Atmosphere. 2022;13:1230. https://doi.org/10.3390/atmos13081230

[19] Statement on the evidence for differential health effects of particulate matter according to source or components. Committee on the Medical Effects of Air Pollutants, 2015.

[20] Zimakowska-Laskowska M, Laskowski P. Comparison of pollutant emissions from various types of vehicles. Combustion Engines. 2024;197(2):139-145. https://doi.org/10.19206/CE-181193

Paula Kurzawska-Pietrowicz, MEng. – Faculty of Civil and Transport Engineering, Poznan University of Technology, Poland.
e-mail: *paula.kurzawska@put.poznan.pl*